Exploring Scaling Laws of CTR Model for Online Performance Improvement

Weijiang Lai
Institute of Software, Chinese Academy of Sciences
University of Chinese Academy of Sciences, Beijing, China
laiweijiang22@otcaix.iscas.ac.cn

Beihong Jin[†]
Institute of Software, Chinese Academy of Sciences
University of Chinese Academy of Sciences, Beijing, China
Beihong@iscas.ac.cn

Jiongyan Zhang
Meituan
Beijing, China
zhangjiongyan@meituan.com

Yiyuan Zheng
Institute of Software, Chinese Academy of Sciences
University of Chinese Academy of Sciences, Beijing, China
zhengyiyuan22@otcaix.iscas.ac.cn

Jian Dong
Meituan
Beijing, China
dongjian03@meituan.com

Jia Cheng
Meituan
Beijing, China
jia.cheng.sh@meituan.com

Jun Lei
Meituan
Beijing, China
leijun@meituan.com

Xingxing Wang
Meituan
Beijing, China
wangxingxing04@meituan.com

Abstract

Click-Through Rate (CTR) models play a vital role in improving user experience and boosting business revenue in many online personalized services. However, current CTR models generally encounter bottlenecks in performance improvement. Inspired by the scaling law phenomenon of Large Language Models (LLMs), we propose a new paradigm for improving CTR predictions: first, constructing a CTR model with accuracy scalable to the model grade and data size, and then distilling the knowledge implied in this model into its lightweight model that can serve online users. To put it into practice, we construct a CTR model named SUAN (**S**tacked **U**nified **A**ttention **N**etwork). In SUAN, we propose the unified attention block (UAB) as a behavior sequence encoder. A single UAB unifies the modeling of the sequential and non-sequential features and also measures the importance of each user behavior feature from multiple perspectives. Stacked UABs elevate the configuration to a high grade, paving the way for performance improvement. In order to benefit from the high performance of the high-grade SUAN and avoid the disadvantage of its long inference time, we modify the SUAN with sparse self-attention and parallel inference strategies to form LightSUAN, and then adopt online distillation to train the low-grade LightSUAN, taking a high-grade SUAN as a teacher. The distilled LightSUAN has superior performance but the same inference time as the LightSUAN, making it well-suited for online deployment. Experimental results show that SUAN performs exceptionally well and holds the scaling laws spanning three orders of magnitude in model grade and data size, and the distilled LightSUAN outperforms the SUAN configured with one grade higher. More importantly, the distilled LightSUAN has been integrated into an online service, increasing the CTR by 2.81% and CPM by 1.69% while keeping the average inference time acceptable. Our source code is available at https://github.com/laiweijiang/SUAN.

[†] Corresponding author.

CCS Concepts

• **Information systems** → **Recommender systems**; **Online advertising**; **Learning to rank**.

Keywords

CTR Prediction, User Modeling, Scaling Law

ACM Reference Format:
Weijiang Lai, Beihong Jin[†], Jiongyan Zhang, Yiyuan Zheng, Jian Dong, Jia Cheng, Jun Lei, and Xingxing Wang. 2025. Exploring Scaling Laws of CTR Model for Online Performance Improvement. In *Proceedings of the Nineteenth ACM Conference on Recommender Systems (RecSys '25), September 22–26, 2025, Prague, Czech Republic.* ACM, New York, NY, USA, 10 pages. https://doi.org/10.1145/3705328.3748046

1 Introduction

The Click-Through Rate (CTR) prediction task in online personalized services is to estimate the probability that a user will click on a desired target, such as an advertisement, a recommended item, or a search result. The CTR prediction requires not only high accuracy but also stringent latency. However, these two requirements conflict with each other, as improvements in accuracy can frequently compromise latency. Therefore, CTR models have been pursuing the goal of pushing the CTR accuracy as high as possible under the tight latency constraint.

So far, a great deal of effort has been dedicated to developing CTR models, often improving performance by analyzing interactions between features and/or sequences of user behaviors. However, current CTR models seem to encounter the performance bottleneck, since in CTR prediction tasks, even a tiny increase of 0.001 in AUC (Area Under the ROC Curve) is regarded as significant [58, 73], where AUC is a widely adopted metric for measuring offline accuracy. Although this viewpoint stems partly from the fact that such a minute increase can yield online gains in the industry, it highlights the difficulty in improving the performance of CTR models.

On the other hand, Large Language Models (LLMs) have been successful in various Natural Language Processing (NLP) tasks [45–47, 51]. Extensive empirical results show that performance of LLMs improves with increasing model size and data size, a phenomenon called scaling laws [50]. Recent practices also indicate that architectures that are based on specific structures, such as self-attention [50, 52] and the mixture of experts [53, 54], exhibit more obvious scaling laws. Meanwhile, various training and inference optimization techniques such as computation reduction and accelerated inference have been proposed to help LLMs land in different scenarios [60–65].

Motivated by the remarkable advancements in LLMs, scaling laws have also been explored in other fields beyond NLP, such as information retrieval [36, 38] and computer vision [34, 35, 37]. Some research has explored the scaling laws in recommender systems [26, 30–33, 56]. However, online services do not gain substantial benefits from the models holding the scaling laws, because these models with high performance cannot be deployed in online services due to the inference time constraint.

In this paper, we present a new paradigm for improving CTR predictions, i.e., we first construct a CTR model with the scaling laws that can get better performance by increasing the model grade and data size, where the model grade, an extension of the concept of model size in the context of scaling laws of models, is defined as the model size plus length of the user behavior sequence fed into the model. This definition is grounded in the consensus that a high-performance CTR model should be able to gain more benefits from longer user behavior sequences while facing rapidly growing user behavior data.

Then, considering that high-grade CTR models have high CTR accuracy but high computational overhead that does not satisfy the inference time constraint, we apply knowledge distillation techniques to transfer the collective knowledge from a high-grade CTR model into a low-grade, more lightweight CTR model. The resulting CTR model is expected to be deployed online and serve users.

Following this line of thought, we propose a CTR model named SUAN (**S**tacked **U**nified **A**ttention **N**etwork) to offer scalable, high-accuracy CTR predictions. Specifically, we design the unified attention block (UAB), which incorporates multiple attention mechanisms to optimize representations of different features, and borrows RMSNorm and SwiGLU from LLMs to enhance training stability. Subsequently, we construct a LightSUAN, a lightweight version of SUAN, and train it using the high-grade SUAN as the teacher. The distilled LightSUAN achieves a performance improvement without compromising inference time and thus can be deployed online.

Our contributions are summarized as follows:

- We design the SUAN model, which comprises stacked UABs. Each UAB is equipped with multiple attention mechanisms: self-attention discerns spatiotemporal dependencies among features within the sequence; cross-attention identifies the significance of user behavior features from the user profile's perspective; and dual alignment attention selectively highlights informative features while suppressing less relevant ones.
- We construct a LightSUAN, i.e., a SUAN with sparse self-attention and parallel inference strategies. Moreover, we adopt online distillation to train the LightSUAN and the high-grade SUAN simultaneously so that the trained LightSUAN can fully leverage the advantages of the high-grade SUAN, essentially allowing it to benefit from the scaling laws held by SUAN.
- We conduct extensive offline experiments on three datasets, and the experimental results show that SUAN not only has excellent AUCs compared to multiple competitors but also holds the AUCs that scale with model grade and data size spanning three orders of magnitude, and the distilled LightSUAN outperforms the original SUAN configured with one grade higher. Moreover, in the online A/B test, the distilled LightSUAN increases the CTR by 2.81%, and CPM by 1.69%, while keeping the average inference time acceptable.

2 Related Work

2.1 CTR Models

CTR models, which perform ranking tasks related to targets, have been a hot topic in both academia and industry.

Currently, CTR models have extensively adopted deep learning technology and can be roughly divided into two categories: one focuses on feature modeling to learn the interactions between features [9, 12, 15, 18, 22, 24, 57**?**] , the other focuses on modeling user behavior sequences to learn user interests and/or intents [19–21, 71, 72].

The first category contains some classic and well-known models. For example, DIN [12] proposes a local activation unit to model the relationship between user behavior and target item, which has a significant impact on the industry. CAN [9] designs a co-action unit that parameterizes the feature embeddings in the form of a micro-MLP to fit complex feature interactions, thereby further enhancing the value of feature interactions.

Most recent progress in CTR models falls into the second category. For example, DSIN [20] introduces sessions into user behavior sequences and employs a bidirectional LSTM [39] to learn the evolution of interests between sessions. BST [21] uses Transformer [49] to learn user behavior sequences. Besides, some CTR models [6–8, 66–70] have focused on modeling long behavior sequences. Industry practices such as SIM [7], ETA [8], and TWIN [6] often adopt a two-stage framework wherein long sequences are first decomposed into multiple short sequences related to the target. These short sequences are then accurately modeled in the second stage. These models can be viewed as a simplified version of a CTR model with scalability of sequence length.

2.2 Scaling Laws in Recommender Systems

Influenced by LLMs, researchers have begun to examine the scaling laws in recommender systems [28, 33].

For sequential recommendation tasks, LSRM [25] and SRT [26] claim that they hold the scaling laws. Both of them adopt the Transformer to encode the user behavior sequences. Specifically, LSRM proposes layer-wise adaptive dropout and switching optimizer strategies to achieve more stable training for large-scale recommendations. SRT adopts pre-training at scale and fine-tuning for downstream tasks to improve performance.

For CTR prediction tasks, simply expanding parameters (such as embedding dimension or parameters of the prediction layer) in CTR models has been found to be insufficient for scalability [29, 30]. To achieve the scaling laws for CTR predictions, Guo et al. [30] propose to learn multiple embeddings for a feature, thus forming the basis of scaling up the performance. Zhang et al. [31] propose the Wukong layer for feature interaction, which consists of a factorization machine block and a linear compress block, performing high-order and second-order feature interactions, respectively. Zhai et al. [32] propose the HSTU architecture to model user behavior sequences for retrieval or ranking tasks. HSTU claims that it has performance scalability w.r.t. training FLOPs whose changes arise from variations in the number of layers, sequence lengths, embedding dimensions, etc. Unfortunately, so far, the way to benefit from CTR models with scaling laws under limited inference time constraints has not been explored in depth.

Compared to existing work, our work not only proposes the key module for obtaining the scaling laws of CTR models but also provides an approach to allowing an online service to benefit from a CTR model with the scaling laws.

3 Methodology

3.1 Overview

Given a user u, his/her behavior sequence containing L behaviors is denoted by $S = \{b_i\}_{i=1}^{L}$, where b_i denotes the i-th behavior, including features such as item ID and timing of behavior. His/Her user profile is denoted by p, with features such as user age and gender. For a candidate c w.r.t. the user u, it includes regular features such as item ID, exposure time, and detailed features such as its CTR of the last 3 days.

Our goal is to build a model that predicts the probability of user u clicking c, that is, $\mathcal{P}(c|S, p) = F(S, p, c; \theta)$, where F denotes our model, and θ denotes the model parameters.

For this goal, we propose a model named SUAN, as illustrated in Figure 1, which consists of an input layer, l UABs as encoders and a prediction layer, where l is the number of UABs.

Since item IDs are numerous, sparse, and often become invalid or outdated compared to NLP tokens, we concatenate regular features of behaviors, such as item ID and category ID, to feed into the input layer. This approach alleviates sparsity and provides collaborative information, enabling better modeling of user interests. Additionally, we append the candidate's regular features to the user behavior sequence to form a target-aware sequence, still using L to denote length for simplification. It helps the encoder understand the relationships between user behaviors and the candidate, enabling the model to focus on behaviors more relevant to the candidate, which is highly beneficial for CTR tasks.

In the input layer, we use a uniform embedding table to initialize target-aware sequence embedding matrix $E_s \in \mathbb{R}^{L \times n_1 d}$, user profile embedding matrix $E_p \in \mathbb{R}^{n_2 \times d}$ and other detailed features embedding vector $e_{other} \in \mathbb{R}^{n_3 d}$, where n_1, n_2, n_3 are the numbers corresponding to features, and d is the dimension.

Within the l UABs, each block models the target-aware sequence via various attention mechanisms, capturing complex relationships and patterns within the sequence, as detailed in Section 3.2.

In the prediction layer, the candidate representation from the final UAB's output $E_{block}[-1, :]$, along with the vector e_p obtained by flattening E_p and other features e_{other} are fed into the multi-layer perception (MLP), and the probability of clicking the candidate $\hat{y}$ is predicted as follows:

$$\hat{y} = \sigma(z), \quad z = \text{MLP}(E_{\text{block}}[-1, :], e_p, e_{\text{other}}), \tag{1}$$

where σ is the sigmoid function and z denotes the logits.

We employ the standard binary cross-entropy loss, denoted as $L_{ce}(\hat{y}, y)$, to optimize our model, where y denotes the ground truth of $\hat{y}$.

3.2 Unified Attention Block

We propose the UAB as a causal encoder, adopting self-attention as its backbone.

At the start of UAB, we apply a pre-norm strategy to normalize the target-aware sequence embedding E_s, as follows:

$$E_{\text{norm}} = \text{RMSNorm}(E_s), \tag{2}$$

where RMSNorm [44] is a variant of layer normalization that utilizes only the root mean square for layer normalization. This strategy, commonly used in LLMs, is introduced into CTR prediction for the first time, serving as a regularizer to reduce computation and maintain training stability.

A complete UAB, in addition to the RMSNorm, includes the self-attention layer, adaptive fusion network (AFNet), and feedforward network (FFN) to discover the importance of features from various perspectives, thereby enhancing the model's expressiveness.

3.2.1 Self-attention Layer. To model target-aware sequences, we use the self-attention mechanism to identify key behaviors, thereby capturing user interests. Specifically, we add the attention bias [32, 59] to the scaled dot-product attention scores to learn the relative positional and temporal relationships between elements. In this layer, we feed with the normalized target-aware sequence embedding E_{norm} to obtain the self-augmented sequence embedding E_{self} as follows:

$$Q_1, K_1, V_1 = E_{\text{norm}} W_1^Q, E_{\text{norm}} W_1^K, E_{\text{norm}} W_1^V, \tag{3}$$

$$\text{bias}_{ij} = f_1(\Delta t_{ij}) + f_2(\Delta p_{ij}), \ i, j \in \{1, 2, \ldots, L\}, \tag{4}$$

$$\text{Attention}(Q_1, K_1, V_1) = \text{softmax}\left(\frac{Q_1 K_1^T}{\sqrt{n_1 d}} + \text{bias}\right) V_1, \tag{5}$$

$$E_{\text{self}} = \text{Concat}(\text{Attention}_1, \ldots, \text{Attention}_h) W_1^O, \tag{6}$$

where $W_1^Q, W_1^K, W_1^V, W_1^O \in \mathbb{R}^{n_1 d \times n_1 d}$ are projection matrices. Δt_{ij} and Δp_{ij} donate the relative time and relative position difference between the $i-$th and the $j-$th elements, respectively, and $f_1(\cdot)$, $f_2(\cdot)$

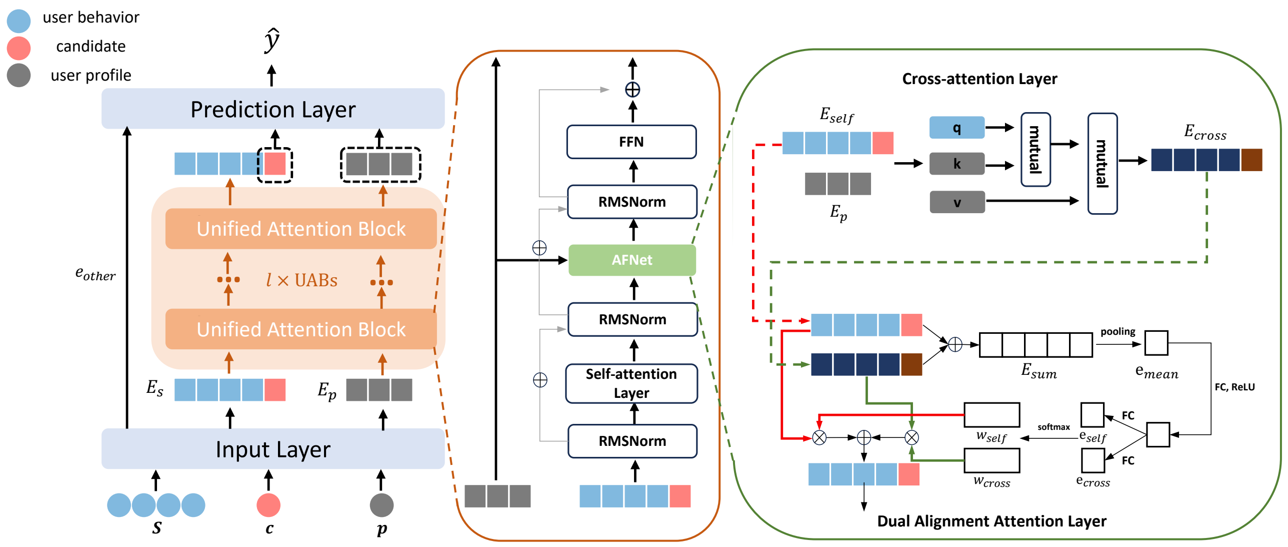

Figure 1: Architecture of SUAN.

are mapping functions that project the difference into learnable variables. h is the number of attention heads. Since there are no obviously temporal or associative relationships among user profile features, such as user age and gender, we opt not to encode them using the self-attention layer for efficiency.

3.2.2 *Adaptive Fusion Network.*

To facilitate effective interaction between sequential and non-sequential features while maintaining feature space consistency, we propose the AFNet, which uniformly models user sequential and non-sequential features. Specifically, AFNet includes a cross-attention layer and a dual alignment attention layer. The cross-attention layer learns the relationship between sequential and non-sequential features to generate the cross-augmented sequence embedding. The dual alignment attention adaptively aligns self-augmented sequence embedding and cross-augmented sequence embedding from the perspective of the global distribution of features.

Cross-attention layer. In this layer, we design unidirectional cross-attention to analyze user behaviors, with the intention of diminishing noise and highlighting key behaviors from the perspective of the user profile, thereby enhancing the expressiveness of sequence embeddings.

This approach is based on the fact that user profile features typically offer a more accurate representation of the user and effectively reflect their interests than behavior features. Thus, incorporating behavior features into the user profile representation tends to introduce noise, affecting its accuracy. Conversely, the user profile can provide precise information for refining user interests. Specifically, we take the self-augmented sequence embedding E_{self} as query and user profile embedding E_p as key and value to obtain the cross-augmented sequence embedding E_{cross}, as shown below:

$$Q_2, K_2, V_2 = E_{\text{self}} W_2^Q, E_p W_2^K, E_p W_2^V, \tag{7}$$

$$\text{Attention}(Q_2, K_2, V_2) = \text{softmax}\left(\frac{Q_2 K_2^T}{\sqrt{n_1 d}}\right) V_2, \tag{8}$$

$$E_{\text{cross}} = \text{concat}(\text{Attention}_1, \ldots, \text{Attention}_h) W_2^O, \tag{9}$$

where $W_2^Q, W_2^O \in \mathbb{R}^{n_1 d \times n_1 d}, W_2^K, W_2^V \in \mathbb{R}^{d \times n_1 d}$ are projection matrices.

Dual Alignment Attention Layer. The self-augmented sequence embedding E_{self} and the cross-augmented sequence embedding E_{cross} aggregate internal behavior relationships and external profile semantics, respectively. In this layer, we combine them to capture comprehensive user interests. For each behavior, the importance of other behaviors and profile contexts differs, making it essential to learn the significance of individual self-augmented and cross-augmented features. Inspired by the channel-wise attention[41, 42], we propose dual alignment attention to align user behavior and profile information for each behavior adaptively. We first generate dimension-wise statistics e_{mean} using global mean pooling as follows:

$$E_{sum} = E_{self} + E_{cross}, \tag{10}$$

$$e_{mean} = \frac{1}{L} \sum_{i=1}^{L} E_{sum}(i, :). \tag{11}$$

Furthermore, we utilize two fully connected (FC) layers to implement the gating mechanism: the first layer suppresses less useful features, and the second layer selectively emphasizes informative features, as demonstrated in the following formulas:

$$e_{self}, e_{cross} = (\rho(e_{mean} W_1)) W_2, (\rho(e_{mean} W_1)) W_3, \tag{12}$$

$$w = \text{softmax}\left(\left[\begin{array}{c} e_{self} \\ e_{cross} \end{array}\right]\right) \in \mathbb{R}^{2 \times L \times n_1 d}, \tag{13}$$

$$w_{self}, w_{cross} = w[0, :, :], w[1, :, :], \tag{14}$$

where ρ is ReLU activation function, and $W_1 \in \mathbb{R}^{n_1 d \times \frac{n_1 d}{4}}, W_2, W_3 \in \mathbb{R}^{\frac{n_1 d}{4} \times n_1 d}$. Next, we obtain the comprehensive user sequence embedding E_{AFN} by the following formula:

$$E_{AFN} = w_{self} \odot E_{self} + w_{cross} \odot E_{cross}. \tag{15}$$

In short, in this layer, we dynamically integrate self-augmented sequence embedding and cross-augmented sequence embedding by perceiving the relationships between user behavior and user profile, and the global feature distribution in the sequence.

3.2.3 Feedforward Network. We adopt SwiGLU-based feedforward network (FFN), which is formulated as follows:

$$E_{FFN} = (\phi(E_{AFN} W_1^{FFN}) \odot E_{AFN} W_2^{FFN}) W_3^{FFN}, \tag{16}$$

where ϕ is the Swish activation function [14], $W_1^{FFN}, W_2^{FFN} \in \mathbb{R}^{n_1 d \times 3 n_1 d}$, $W_3^{FFN} \in \mathbb{R}^{3 n_1 d \times n_1 d}$. The FFN combines the property of being differentiable everywhere in the Swish function with the advantage of the gating mechanism in GLU [13]. Similar FFNs are used in LLMs.

3.3 Deployment Optimization

3.3.1 Speedup Strategies. To alleviate the high time complexity of the SUAN model, we adopt sparse self-attention and parallel inference strategies, and the modified model is referred to as LightSUAN.

Sparse self-attention. As we know, the time complexity of the self-attention mechanism is quadratic in the sequence length, which can significantly affect model training and inference times when the sequence length is long. Sparse self-attention seeks to lessen the computational burden by reducing the number of attention connections.

Our sparse self-attention is a combination of local self-attention and dilated self-attention, enabling the effective capture of both recent and distant relationships [11]. In the local self-attention, each element attends only to its neighboring elements within a local window, where k denotes the window size. In the dilated self-attention, each element attends only to every r-th element, where r is the dilated rate. The middle part of Figure 2 shows the method of calculating a sparse self-attention matrix, where $r = 2$ and $k = 2$.

Parallel inference. For a user, online CTR prediction involves ranking multiple candidates. If there are m_1 candidates, then m_1 separate inferences are performed conventionally. Since CTR models have strict requirements for inference time, it is essential to propose a parallel inference strategy to accelerate online inference.

In SUAN, our causal encoder ensures that behavior representations are independent of candidate representations, which enables parallel inference through the reuse of behavior representations. Our parallel inference strategy requires modifications to online inference and offline training. For online inference, since the value of m_1 is variable in a specific online service, we input m_2 ($m_2 < m_1$) candidates for parallel inference, obtaining m_2 results in a separate inference. This reduces the number of inferences to $\lceil m_1/m_2 \rceil$ per user. To match the online parallel inference, we modify the implementation specifics of offline training to simulate the online scenario. First, we modify the training samples to ensure consistency with the input of the online inference. To be specific, for an original training sample that includes only a single candidate, we append $m_2 - 1$ placeholders to this candidate. Then, we modify the method of calculating the attention matrix. The right part of Figure 2 shows an example illustrating how to perform parallel inference in conjunction with the sparse self-attention mechanism, where $k = 2$, $r = 2$, and $m_2 = 3$.

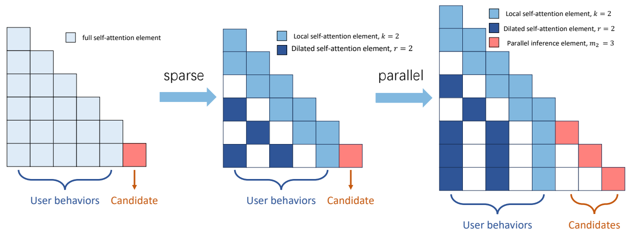
full self-attention element
sparse
Local self-attention element, $k = 2$
Dilated self-attention element, $r = 2$
parallel
Local self-attention element, $k = 2$
Dilated self-attention element, $r = 2$
Parallel inference element, $m_2 = 3$
User behaviors
Candidate
User behaviors
Candidate
User behaviors
Candidates

Figure 2: Illustration of self-attention matrix in LightSUAN.

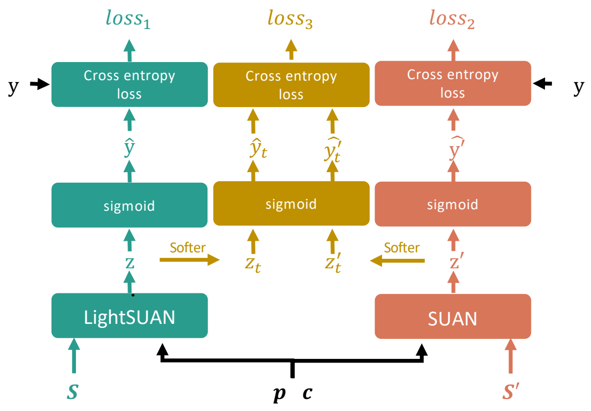

Figure 3: Illustration of online distillation.

3.3.2 Online distillation. To efficiently transfer knowledge from a high-grade SUAN to a deployable low-grade LightSUAN, we design an online distillation approach that trains these two models simultaneously after examining various distillation techniques [1–5].

As illustrated in Figure 3, a low-grade LightSUAN acts as a student, fed with S, c, p, and a high-grade SUAN acts as a teacher, fed with S', c, p. $\hat{y}$ and $\hat{y'}$ denote the predication probabilities and z and z' denote the logits output by two models. Besides, $z_t = z/t$, $z'_t = z'/t$ where t denotes a temperature, resulting in softer probability distributions over classes. Further, $\hat{y}_t = \sigma(z_t), \hat{y'_t} = \sigma(z'_t)$. We optimize two models using three binary cross-entropy loss functions: $loss_1 = L_{ce}(\hat{y}, y)$, $loss_2 = L_{ce}(\hat{y'}, y)$, and $loss_3 = L_{ce}(\hat{y}_t, \hat{y'_t})$, where $\hat{y'_t}$ acts as a soft label.

The final loss for the online distillation is as follows:

$$loss = loss_1 + loss_2 + \lambda loss_3, \tag{17}$$

where λ is the weight coefficient for the distillation loss. Since magnitudes of the gradients produced by $loss_3$ scale as $1/t$ [1], we set λ to t to counterbalance this scaling, ensuring that $loss_3$ contributes appropriately to the overall gradient during the optimization process.

3.4 Complexity Analysis

3.4.1 Time complexity. SUAN's time complexity primarily comes from the self-attention and cross-attention layers within the UAB. The primary complexity for l UABs with full attention is $O(BlL^2 n_1 d + BlLn_2 n_1 d)$, where B is the batch size.

In LightSUAN, we adopt the sparse self-attention to reduce the time complexity to $O(BlL(k + \frac{L}{r}) n_1 d + BlLn_2 n_1 d)$. Furthermore, we

Table 1: Statistics of the datasets.

Dataset	#Users	#Items	#Samples
Eleme	14,427,689	7,446,116	128,000,000
Taobao	1,141,729	461,527	700,000,000
Industry	88,976,000	14,054,691	1,230,715,133

use the parallel inference strategy to decrease the inference time per user from $O(m_1(BlL(k+\frac{L}{r})n_1d+BlLn_2n_1d))$ to $O(\frac{m_1}{m_2}(Bl(L+m_2)(k+\frac{L+m_2}{r})n_1d+Bl(L+m_2)n_2n_1d))$.

3.4.2 Space complexity. In addition to embeddings, the extra learnable parameters in our model primarily come from the UABs, which include the self-attention layer, AFNet, and FFN, their learnable parameters are $O(4ln_1^2d^2)$, $O(l(2n_1^2d^2+2n_1n_2d^2+\frac{3n_1^2d^2}{4}))$ and $O(9ln_1^2d^2)$, respectively.

4 Experiments

4.1 Experimental Settings

4.1.1 Datasets. We adopt two public datasets and one industrial dataset to conduct experiments. **Eleme**[1] is constructed from logs of the Ele.me service and contains 30-day behaviors of users. It has abundant behavior features, including item features and behavior features. **Taobao**[2] is collected from the display advertising system in Alibaba and contains 22-day behaviors of nearly a million randomly chosen users on Taobao. Each user behavior has a behavior type, the time when behavior has occurred, and so on. **Industry** is an industrial dataset that contains up to 1000 behavioral records from the past year for each of 88 million users who are sampled from active users during the 7-day period from July 6, 2024, to July 12, 2024. Each user behavior includes item features and behavior features. The statistics of three datasets are shown in Table 1.

4.1.2 Competitors. We choose eight methods of different research lines as competitors. Two of them, i.e., **DIN** [12] and **CAN** [9], focus on modeling behavior feature interactions (assigned to Group I), and the other six, i.e., **SoftSIM**, **HardSIM**, **ETA** [8], **TWIN** [6], **BST** [21] and **HSTU** [32], adopt behavior sequence modeling, where **SoftSIM** and **HardSIM** are two variants of **SIM** [7], using the embedding similarity retrieval and category retrieval, respectively. Of these six methods, the first four are designed for long sequences (assigned to Group II), and the last two are not (Group III).

4.1.3 Evaluation Metrics. In the offline experiments, we adopt AUC as an evaluation metric. Besides, we follow [12, 40] to introduce the relative improvement (RelaImpr) metric to measure relative improvement between models. In the online A/B test, we adopt CTR, Cost Per Mille (CPM) and inference time as evaluation metrics.

4.1.4 Implementation Details. We implement all models by TensorFlow. For the sake of fairness, all models are configured to have parameters of the same order of magnitude. Specifically, the dimension of all models is set to 8, and the same prediction layer was set for all models, i.e., the MLP structure in the prediction layer is [1024, 512, 256, 1], using the Dice as the activation function. Meanwhile, for our model and the models in Group III, we set their encoder layers to 2 and the attention heads to 2. During distillation, the hyperparameters t and λ are set to 2.

In addition, for the industrial dataset and Taobao dataset, we set the sequence length to 1000 for the models in Group II and 100 for the models in Groups I and III. Due to limitations of the Eleme dataset, we set the sequence length to 50 for the models in Group II and 10 for the models in Groups I and III. Moreover, in addition to SUAN, which is set to the same sequence length as the models in Group I, we also employ SUAN(L), i.e., the SUAN with the same sequence length as the models in Group II, to evaluate the performance of our model on long sequences.

We train all models on NVIDIA A100-80G. We train each of them for one epoch, using Adam as the optimizer.

4.2 Overall Performance

The performance evaluation results are listed in Table 2. We also conduct a t-test on the AUCs of our model and each comparison model, while setting a significance level to 0.05. All p-values are less than 0.05, indicating a statistically significant difference between our model and the other models in terms of AUC.

From the results, we find that the CTR models for long sequences outperform DIN and CAN, indicating that incorporating longer user behaviors helps learn more comprehensive user interests, which is beneficial for CTR predictions. Compared to the CTR models for long sequences, the CTR models in Group III and SUAN take shorter user behavior sequences as input, but perform better. There likely exist two reasons. First, the models in Group II decompose a long sequence into short subsequences, potentially losing valuable information that is implied in the long sequence. Second, the models in Group III and SUAN utilize the self-attention mechanism to analyze user behaviors and learn the relationships between those behaviors, thereby gaining a better understanding of user interests.

Last and most importantly, our model significantly outperforms all competitors on three datasets. The results from column SUAN(L) also demonstrate that our model can further enhance its performance by taking longer sequences as input.

4.3 Ablation Study

We construct five variants to evaluate the effectiveness of the modules in SUAN. Variants A, B are the models that remove SwiGLU and AFNet from UAB, respectively. Variant C is to replace dual alignment attention in AFNet with a simple strategy that directly combines the self-augmented sequence embedding and cross-augmented sequence embedding using addition. Variant D is the model that replaces the target-aware sequence in SUAN with a pure user behavior sequence and is directly fed with the candidate's feature representations in the prediction layer. In other words, variant D abandons the target-aware sequence in SUAN. Variant E simplifies UAB by removing the attention bias of the self-attention layer.

The results are shown in Table 3. Compared to SUAN, all these variants exhibit varying degrees of performance degradation, illustrating the effectiveness of the designed modules. Especially, variant D shows substantial performance deterioration, highlighting that the target-aware sequence, which exploits the distinctiveness of the

[1]https://tianchi.aliyun.com/dataset/131047
[2]https://tianchi.aliyun.com/dataset/56

Table 2: Performance comparison. We repeat each experiment three times and report the average results. We also report the standard deviation of SUAN's results. In each row, the best and second-best results are highlighted in bold, and the third-best results are underlined. DIN is considered the base model for calculating the RelaImpr.

Dataset	Metric	Group I		Group II				Group III			
		DIN	CAN	SoftSIM	HardSIM	ETA	TWIN	BST	HSTU	SUAN	SUAN(L)
Industry	AUC	0.7002	0.7004	0.7025	0.7020	0.7024	0.7028	0.7028	<u>0.7036</u>	**0.7098**±0.00004	**0.7135**±0.00048
	RelaImpr	0.00%	0.10%	1.15%	0.90%	1.10%	1.30%	1.30%	<u>1.70%</u>	**4.80%**±0.02%	**6.64%**±0.24%
Eleme	AUC	0.6363	0.6378	0.6399	0.6389	0.6398	0.6410	0.6600	<u>0.6631</u>	**0.6669**±0.00028	**0.6690**±0.00090
	RelaImpr	0.00%	1.10 %	2.64%	1.90%	2.56%	3.44%	17.38%	<u>19.66%</u>	**22.45%**±0.21%	**23.99%**±0.66%
Taobao	AUC	0.6198	0.6184	0.6212	0.6239	0.6220	0.6215	0.6370	<u>0.6397</u>	**0.6472**±0.00011	**0.6495**±0.00088
	RelaImpr	0.00%	-1.17%	1.17%	3.42%	1.84%	1.42%	14.36%	<u>16.61%</u>	**22.87%**±0.09%	**24.97%**±0.73%

Table 3: Results of the ablation study.

Model	Industry	Eleme	Taobao
SUAN	0.7098	0.6669	0.6472
Variant A	0.7093	0.6644	0.6468
Variant B	0.7075	0.6644	0.6431
Variant C	0.7080	0.6652	0.6441
Variant D	0.7042	0.6638	0.6434
Variant E	0.7040	0.6631	0.6433

Table 4: Configurations of model sizes.

Model Size	d	l	h	#Non-embedding Parameters
size-1	8	1	1	2,929,118
size-2	8	2	2	3,050,358
size-3	16	4	4	4,102,838
size-4	32	8	8	10,824,646
size-5	144	12	12	129,363,030

CTR prediction task, plays a significant role in improving performance. Variant E has the greatest decline in performance, indicating that the relative position and temporal information between behaviors are crucial for learning relationships among behaviors.

4.4 Scaling Law Analysis

Similar to existing studies on scaling laws [50, 53–55], the way to determine whether the scaling law phenomenon exists in our model is by examining the effect of model grade and data size on model performance. In SUAN, the model grade is determined by two factors: the model size and behavior sequence length, where model size typically refers to the number of non-embedding parameters, which are primarily influenced by the dimension d, and the parameters l and h of the UBA in SUAN. The data size refers to the number of samples that are input into the model. Unlike existing studies focusing on the loss values [25, 50], our exploration is more concerned with AUC, as this metric is more valuable than the loss value in CTR prediction scenarios. Limited by the data size of public datasets, we conduct experiments on the industrial dataset.

4.4.1 Impact of Scaling the Model Grade. We take 7-day samples as input, and run SUAN under different combinations of model size and sequence length, where the model size is set according to Table 4 and the sequence length is selected from {50, 100, 200, 500, 1000}. For each combination, we calculate the AUC.

Taking inspiration from [26, 27], we propose fitting the AUCs into a power-law function $AUC(C) = E_1 - A_1/(C - B_1)^{\alpha}$, where C is the number of non-embedding parameters, E_1, A_1, B_1, and α are the coefficients to be fitted. E_1 can be explained as the potential upper bound of AUC values. B_1 can be understood as the number of parameters not tied to the scaling laws in the CTR prediction task, such as the parameters in the prediction layer. We apply the least squares method to fit AUCs into a nonlinear curve. The results are displayed in Figure 4a. The coefficients of determination (R^2) are close to 1, which indicates that the fits are of high quality. From the results, we confirm that, while fixing data size, AUCs of SUAN adhere to a power-law function with respect to model size across different sequence lengths.

Much like AUC(C), we employ $AUC(L) = E_2 - A_2/L^{\beta}$ to investigate the relationship between the AUC value and sequence length, where L denotes the sequence length, and E_2, A_2, and β are the coefficients. The fitted curves and formulas are shown in Figure 4b, confirming that when given fixed-size data as input, a scaling law holds when the sequence length varies.

From the results of AUC(C) and AUC(L) in Figure 4, we find that the values of E_1 and E_2 are both approximately 0.72, indicating that an upper bound does exist for the AUC improvement under a fixed data size.

4.4.2 Impact of Scaling the Data Size. We choose three models, i.e., SUAN, HSTU, and DIN, whose configurations are identical to those in Section 4.1.4. For each model, we fix its configuration and run the model using different numbers of samples as input. Here, samples are collected from {3, 7, 14, 30, 45, 90} days, and the number of samples spans three orders of magnitude from 3.43×10^8 to 2×10^{10}. We calculate the AUC for each run of the model, and then fit AUCs using $AUC(D) = E_3 - A_3/D^{\gamma}$, where D is the number of samples, and E_3, A_3, and γ are the coefficients to be estimated. The curves and formulas are shown in Figure 4c. We find that the power-law function of SUAN exhibits a higher E_3 and a smaller γ value compared to HSTU and DIN. This implies that our model

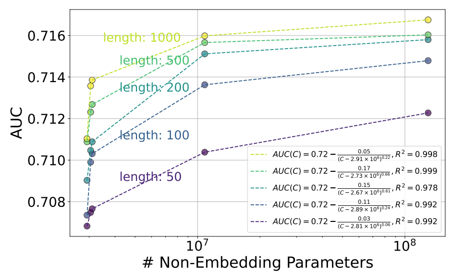

(a)

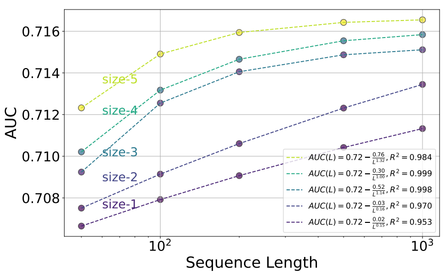

(b)

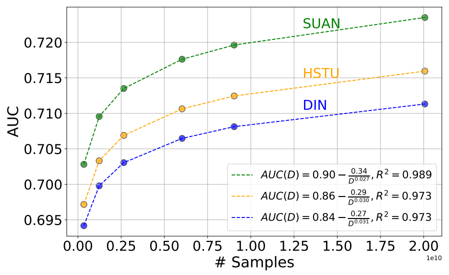

(c)

Figure 4: Scaling laws on the industrial dataset: (a) Model sizes, (b) Sequence lengths, and (c) Data size.

Table 5: Performance of models with different model sizes.

Model	size-2	size-4
SUAN	0.7098±0.00004	0.7133±0.00128
Variant F	0.7092±0.00068	0.7097±0.00331
Variant G	0.7097±0.00019	0.7064±0.00463

can utilize training samples more effectively and exhibits excellent scalability across various data scales.

Furthermore, we find that E_3 values are higher than E_2 and E_1 values, and γ values are lower than both α and β values. This means that increasing the data size, as opposed to the model grade, achieves a higher upper bound and a faster growth rate of AUC for our model.

4.4.3 Regularizers for Supporting Scaling Laws. We set up two configurations that differ only in model size, and run SUAN and all variants A through G three times under each configuration, observing their AUC discrepancies, where variant F replaces RMSNorm with standard Layer-Norm, and variant G replaces the pre-norm strategy with the post-norm strategy.

We find that only variants F and G with a model size of size-4 exhibit performance degradation, as indicated by their mean AUCs and standard deviations shown in Table 5. Their performance undermines the scaling law. We attribute these results to RMSNorm using the root mean square for layer normalization, which better reduces the impact of outliers and mitigates abnormal gradients, maintaining training stability. Further, pre-norm applies normalization at the start of the UAB, reducing numerical instability from subsequent complex operations. Conversely, post-norm normalizes after all UAB operations, which can easily cause gradient vanishing or explosion in deep models.

Based on these findings, we reasonably speculate that the RMSNorm and pre-norm strategies are beneficial for maintaining the scaling law, preventing outliers and fluctuations from destroying the scaling laws.

4.5 Deployment Optimization Analysis

4.5.1 The impact of sparse self-attention. We choose the LightSUAN whose model size is set to size-2 and window size k to 2, and observe inference speeds and AUCs on the industrial dataset across different dilated rates r and sequence lengths, where the LightSUAN with $r = 1$ is degenerated into the original SUAN with full attention.

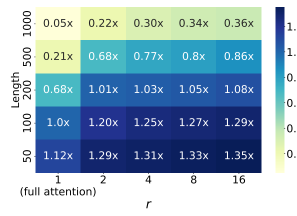

(a)

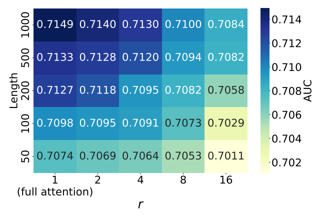

(b)

Figure 5: The impact of sparse self-attention on the model's (a) Efficiency, and (b) Performance.

Figure 5a shows the relative inference speed with respect to the unit inference speed across varying dilated rates and sequence lengths, where the unit inference speed is calculated based on the time spent in inference for the model with full attention and a sequence length of 100. The results in Figure 5a illustrate that inference speed notably increases as the dilated rate increases. Figure 5b gives the AUC values under different dilated rates and sequence lengths. From the results in Figure 5b, it can be seen that there is no significant performance drop when $r <= 4$ and AUC boosts rapidly as the sequence length grows longer.

4.5.2 The impact of online distillation. We first train one deployable low-grade LightSUAN and three high-performance high-grade SUAN models that are unable to be deployed online due to their long inference times. Table 6 details their configurations and AUCs on the industrial dataset. We then adopt online distillation to obtain three distilled LightSUAN models. Table 7 shows the distilled models and their AUCs on the industrial dataset.

The results reveal that distilled models can obtain enhanced performance. Notably, DistilSUAN-3 outperforms LightSUAN-1 by 6‰ and also exceeds the performance of both SUAN-1, which is equipped with a larger model size, and SUAN(L), which takes a longer sequence as input, as shown in Table 2.

4.6 Online A/B Test

We conducted an online A/B test that lasted for three weeks. Considering the limited computational budget and the constraint on online inference time, we deploy the original SUAN with a model

Table 6: Details of models. More ⋆s indicate a higher grade.

Model	Model Size	Length	Grade	Sparse	AUC
LightSUAN-1	size-2	100	⋆	r=2, k=2	0.7095
SUAN-1	size-4	100	⋆⋆	-	0.7133
SUAN-2	size-4	200	⋆⋆⋆	-	0.7146
SUAN-3	size-5	1000	⋆⋆⋆⋆	-	0.7168

Table 7: Performance comparison of distilled models.

Distilled Model	Low-grade Model (as student)	High-grade Model (as teacher)	AUC
DistilSUAN-1	LightSUAN-1	SUAN-1	0.7114
DistilSUAN-2		SUAN-2	0.7122
DistilSUAN-3		SUAN-3	0.7139

size of size-2 and sequence length of 100, and DistilSUAN-3 in the live production environment of an online service, providing list advertisement recommendations. The baseline is the original online-serving CTR model, which has undergone several rounds of model upgrades, getting the essence from multiple basic models, including DIN, CAN, SIM, and other multi-behavior models.

Compared to the baseline, the original SUAN improves CTR by 2.67% and CPM by 1.63%, with an increase in average inference time from 33ms to 48ms, and the distilled LightSUAN enhances CTR by 2.81% and CPM by 1.69%, achieving this with an average inference time of 43ms.

5 Conclusion

This paper explores the potential of modeling user behaviors to make CTR prediction performance conform to the scaling laws and presents a knowledge distillation approach to allowing an online service to benefit from a CTR model with scaling laws. This study not only offers new insights into CTR predictions to support online performance improvement in the industry but also shares hands-on experience in identifying factors (e.g., model grade) and components (e.g., regularizers) affecting scaling laws of the CTR model.

Acknowledgments

This work was supported by the National Natural Science Foundation of China under Grant No. 62072450 and Meituan.

References

[1] G. Hinton, O. Vinyals, and J. Dean, "Distilling the knowledge in a neural network," *arXiv preprint arXiv:1503.02531*, 2015.

[2] C. Buciluǎ, R. Caruana, and A. Niculescu-Mizil, "Model compression," in *Proceedings of the 12th ACM SIGKDD international conference on Knowledge discovery and data mining*, 2006, pp. 535–541.

[3] Y. Zhang, T. Xiang, T. M. Hospedales, and H. Lu, "Deep mutual learning," in *2018 IEEE/CVF Conference on Computer Vision and Pattern Recognition.* IEEE, 2018, pp. 4320–4328.

[4] D. Chen, J.-P. Mei, C. Wang, Y. Feng, and C. Chen, "Online knowledge distillation with diverse peers," in *Proceedings of the AAAI conference on artificial intelligence*, vol. 34, no. 04, 2020, pp. 3430–3437.

[5] N. Khani, L. Wei, A. Nath, S. Andrews, S. Yang, Y. Liu, P. Abbo, M. Kula, J. Kahn, Z. Zhao *et al.*, "Bridging the gap: Unpacking the hidden challenges in knowledge distillation for online ranking systems," in *Proceedings of the 18th ACM Conference on Recommender Systems*, 2024, pp. 758–761.

[6] J. Chang, C. Zhang, Z. Fu, X. Zang, L. Guan, J. Lu, Y. Hui, D. Leng, Y. Niu, Y. Song *et al.*, "Twin: Two-stage interest network for lifelong user behavior modeling in ctr prediction at kuaishou," in *Proceedings of the 29th ACM SIGKDD Conference on Knowledge Discovery and Data Mining*, 2023, pp. 3785–3794.

[7] Q. Pi, G. Zhou, Y. Zhang, Z. Wang, L. Ren, Y. Fan, X. Zhu, and K. Gai, "Search-based user interest modeling with lifelong sequential behavior data for click-through rate prediction," in *Proceedings of the 29th ACM International Conference on Information & Knowledge Management*, 2020, pp. 2685–2692.

[8] Q. Chen, C. Pei, S. Lv, C. Li, J. Ge, and W. Ou, "End-to-end user behavior retrieval in click-through rate prediction model," *arXiv preprint arXiv:2108.04468*, 2021.

[9] W. Bian, K. Wu, L. Ren, Q. Pi, Y. Zhang, C. Xiao, X.-R. Sheng, Y.-N. Zhu, Z. Chan, N. Mou *et al.*, "Can: feature co-action network for click-through rate prediction," in *Proceedings of the fifteenth ACM international conference on web search and data mining*, 2022, pp. 57–65.

[10] R. Child, S. Gray, A. Radford, and I. Sutskever, "Generating long sequences with sparse transformers," *arXiv preprint arXiv:1904.10509*, 2019.

[11] Y. Tay, M. Dehghani, D. Bahri, and D. Metzler, "Efficient transformers: A survey," vol. 55, no. 6, Dec. 2022. [Online]. Available: https://doi.org/10.1145/3530811

[12] G. Zhou, X. Zhu, C. Song, Y. Fan, H. Zhu, X. Ma, Y. Yan, J. Jin, H. Li, and K. Gai, "Deep interest network for click-through rate prediction," in *Proceedings of the 24th ACM SIGKDD international conference on knowledge discovery & data mining*, 2018, pp. 1059–1068.

[13] N. Shazeer, "Glu variants improve transformer," *arXiv preprint arXiv:2002.05202*, 2020.

[14] P. Ramachandran, B. Zoph, and Q. V. Le, "Searching for activation functions," *arXiv preprint arXiv:1710.05941*, 2017.

[15] H. Guo, R. Tang, Y. Ye, Z. Li, and X. He, "Deepfm: a factorization-machine based neural network for ctr prediction," in *Proceedings of the 26th International Joint Conference on Artificial Intelligence*, 2017, pp. 1725–1731.

[16] J. Xiao, H. Ye, X. He, H. Zhang, F. Wu, and T.-S. Chua, "Attentional factorization machines: learning the weight of feature interactions via attention networks," in *Proceedings of the 26th International Joint Conference on Artificial Intelligence*, 2017, pp. 3119–3125.

[17] Y. Yang, B. Xu, S. Shen, F. Shen, and J. Zhao, "Operation-aware neural networks for user response prediction," *Neural Networks*, vol. 121, pp. 161–168, 2020.

[18] H.-T. Cheng, L. Koc, J. Harmsen, T. Shaked, T. Chandra, H. Aradhye, G. Anderson, G. Corrado, W. Chai, M. Ispir *et al.*, "Wide & deep learning for recommender systems," in *Proceedings of the 1st workshop on deep learning for recommender systems*, 2016, pp. 7–10.

[19] G. Zhou, N. Mou, Y. Fan, Q. Pi, W. Bian, C. Zhou, X. Zhu, and K. Gai, "Deep interest evolution network for click-through rate prediction," in *Proceedings of the AAAI conference on artificial intelligence*, vol. 33, no. 01, 2019, pp. 5941–5948.

[20] Y. Feng, F. Lv, W. Shen, M. Wang, F. Sun, Y. Zhu, and K. Yang, "Deep session interest network for click-through rate prediction," in *Proceedings of the 28th International Joint Conference on Artificial Intelligence*, 2019, pp. 2301–2307.

[21] Q. Chen, H. Zhao, W. Li, P. Huang, and W. Ou, "Behavior sequence transformer for e-commerce recommendation in alibaba," in *Proceedings of the 1st international workshop on deep learning practice for high-dimensional sparse data*, 2019, pp. 1–4.

[22] P. Covington, J. Adams, and E. Sargin, "Deep neural networks for youtube recommendations," in *Proceedings of the 10th ACM conference on recommender systems*, 2016, pp. 191–198.

[23] J. Lian, X. Zhou, F. Zhang, Z. Chen, X. Xie, and G. Sun, "xdeepfm: Combining explicit and implicit feature interactions for recommender systems," in *Proceedings of the 24th ACM SIGKDD international conference on knowledge discovery & data mining*, 2018, pp. 1754–1763.

[24] R. Wang, B. Fu, G. Fu, and M. Wang, "Deep & cross network for ad click predictions," in *Proceedings of the ADKDD'17*, 2017, pp. 1–7.

[25] G. Zhang, Y. Hou, H. Lu, Y. Chen, W. X. Zhao, and J.-R. Wen, "Scaling law of large sequential recommendation models," in *Proceedings of the 18th ACM Conference on Recommender Systems*, 2024, pp. 444–453.

[26] P. Zivic, H. Vazquez, and J. Sánchez, "Scaling sequential recommendation models with transformers," in *Proceedings of the 47th International ACM SIGIR Conference on Research and Development in Information Retrieval*, 2024, pp. 1567–1577.

[27] J. Hoffmann, S. Borgeaud, A. Mensch, E. Buchatskaya, T. Cai, E. Rutherford, D. de Las Casas, L. A. Hendricks, J. Welbl, A. Clark *et al.*, "Training compute-optimal large language models," in *Proceedings of the 36th International Conference on Neural Information Processing Systems*, 2022, pp. 30 016–30 030.

[28] S. Chitlangia, K. R. Kesari, and R. Agarwal, "Scaling generative pre-training for user ad activity sequences," in *KDD 2023 Workshop on Artificial Intelligence for Computational Advertising (AdKDD)*, 2023. [Online]. Available: https://www.amazon.science/publications/scaling-generative-pre-training-for-user-ad-activity-sequences

[29] N. Ardalani, C.-J. Wu, Z. Chen, B. Bhushanam, and A. Aziz, "Understanding scaling laws for recommendation models," *arXiv preprint arXiv:2208.08489*, 2022.

[30] X. Guo, J. Pan, X. Wang, B. Chen, J. Jiang, and M. Long, "On the embedding collapse when scaling up recommendation models," in *Proceedings of the 41st International Conference on Machine Learning*, 2024, pp. 16 891–16 909.

[31] B. Zhang, L. Luo, Y. Chen, J. Nie, X. Liu, S. Li, Y. Zhao, Y. Hao, Y. Yao, E. D. Wen *et al.*, "Wukong: towards a scaling law for large-scale recommendation," in *Proceedings of the 41st International Conference on Machine Learning*, 2024, pp.

59 421–59 434.
[32] J. Zhai, L. Liao, X. Liu, Y. Wang, R. Li, X. Cao, L. Gao, Z. Gong, F. Gu, J. He *et al.*, "Actions speak louder than words: trillion-parameter sequential transducers for generative recommendations," in *Proceedings of the 41st International Conference on Machine Learning*, 2024, pp. 58 484–58 509.
[33] K. Shin, H. Kwak, S. Y. Kim, M. N. Ramström, J. Jeong, J.-W. Ha, and K.-M. Kim, "Scaling law for recommendation models: Towards general-purpose user representations," in *Proceedings of the AAAI Conference on Artificial Intelligence*, vol. 37, no. 4, 2023, pp. 4596–4604.
[34] M. Dehghani, J. Djolonga, B. Mustafa, P. Padlewski, J. Heek, J. Gilmer, A. P. Steiner, M. Caron, R. Geirhos, I. Alabdulmohsin *et al.*, "Scaling vision transformers to 22 billion parameters," in *International Conference on Machine Learning*. PMLR, 2023, pp. 7480–7512.
[35] X. Zhai, A. Kolesnikov, N. Houlsby, and L. Beyer, "Scaling vision transformers," in *Proceedings of the IEEE/CVF conference on computer vision and pattern recognition*, 2022, pp. 12 104–12 113.
[36] C. Jia, Y. Yang, Y. Xia, Y.-T. Chen, Z. Parekh, H. Pham, Q. Le, Y.-H. Sung, Z. Li, and T. Duerig, "Scaling up visual and vision-language representation learning with noisy text supervision," in *International conference on machine learning*. PMLR, 2021, pp. 4904–4916.
[37] H. Pham, Z. Dai, G. Ghiasi, K. Kawaguchi, H. Liu, A. W. Yu, J. Yu, Y.-T. Chen, M.-T. Luong, Y. Wu *et al.*, "Combined scaling for zero-shot transfer learning," *Neurocomputing*, vol. 555, p. 126658, 2023.
[38] Y. Fang, J. Zhan, Q. Ai, J. Mao, W. Su, J. Chen, and Y. Liu, "Scaling laws for dense retrieval," in *Proceedings of the 47th International ACM SIGIR Conference on Research and Development in Information Retrieval*, 2024, pp. 1339–1349.
[39] A. Graves and A. Graves, "Long short-term memory," *Supervised sequence labelling with recurrent neural networks*, pp. 37–45, 2012.
[40] L. Yan, W.-J. Li, G.-R. Xue, and D. Han, "Coupled group lasso for web-scale ctr prediction in display advertising," in *International conference on machine learning*. PMLR, 2014, pp. 802–810.
[41] J. Hu, L. Shen, and G. Sun, "Squeeze-and-excitation networks," in *Proceedings of the IEEE conference on computer vision and pattern recognition*, 2018, pp. 7132–7141.
[42] X. Li, W. Wang, X. Hu, and J. Yang, "Selective kernel networks," in *Proceedings of the IEEE/CVF conference on computer vision and pattern recognition*, 2019, pp. 510–519.
[43] G. S. Manku, A. Jain, and A. Das Sarma, "Detecting near-duplicates for web crawling," in *Proceedings of the 16th international conference on World Wide Web*, 2007, pp. 141–150.
[44] B. Zhang and R. Sennrich, "Root mean square layer normalization," *Advances in Neural Information Processing Systems*, vol. 32, 2019.
[45] H. Touvron, T. Lavril, G. Izacard, X. Martinet, M.-A. Lachaux, T. Lacroix, B. Rozière, N. Goyal, E. Hambro, F. Azhar *et al.*, "Llama: Open and efficient foundation language models," *arXiv preprint arXiv:2302.13971*, 2023.
[46] J. Bai, S. Bai, Y. Chu, Z. Cui, K. Dang, X. Deng, Y. Fan, W. Ge, Y. Han, F. Huang *et al.*, "Qwen technical report," *arXiv preprint arXiv:2309.16609*, 2023.
[47] T. B. Brown, B. Mann, N. Ryder, M. Subbiah, J. Kaplan, P. Dhariwal, A. Neelakantan, P. Shyam, G. Sastry, A. Askell *et al.*, "Language models are few-shot learners," in *Proceedings of the 34th International Conference on Neural Information Processing Systems*, 2020, pp. 1877–1901.
[48] G. Klambauer, T. Unterthiner, A. Mayr, and S. Hochreiter, "Self-normalizing neural networks," *Advances in neural information processing systems*, vol. 30, 2017.
[49] A. Vaswani, "Attention is all you need," *Advances in Neural Information Processing Systems*, 2017.
[50] J. Kaplan, S. McCandlish, T. Henighan, T. B. Brown, B. Chess, R. Child, S. Gray, A. Radford, J. Wu, and D. Amodei, "Scaling laws for neural language models," *arXiv preprint arXiv:2001.08361*, 2020.
[51] J. Achiam, S. Adler, S. Agarwal, L. Ahmad, I. Akkaya, F. L. Aleman, D. Almeida, J. Altenschmidt, S. Altman, S. Anadkat *et al.*, "Gpt-4 technical report," *arXiv preprint arXiv:2303.08774*, 2023.
[52] T. Henighan, J. Kaplan, M. Katz, M. Chen, C. Hesse, J. Jackson, H. Jun, T. B. Brown, P. Dhariwal, S. Gray *et al.*, "Scaling laws for autoregressive generative modeling," *arXiv preprint arXiv:2010.14701*, 2020.
[53] A. Clark, D. de Las Casas, A. Guy, A. Mensch, M. Paganini, J. Hoffmann, B. Damoc, B. Hechtman, T. Cai, S. Borgeaud *et al.*, "Unified scaling laws for routed language models," in *International conference on machine learning*. PMLR, 2022, pp. 4057–4086.
[54] J. Ludziejewski, J. Krajewski, K. Adamczewski, M. Pióro, M. Krutul, S. Antoniak, K. Ciebiera, K. Król, T. Odrzygóźdź, P. Sankowski *et al.*, "Scaling laws for fine-grained mixture of experts," in *Forty-first International Conference on Machine Learning*, 2024.
[55] J. Ma, Z. Zhao, X. Yi, J. Chen, L. Hong, and E. H. Chi, "Modeling task relationships in multi-task learning with multi-gate mixture-of-experts," in *Proceedings of the 24th ACM SIGKDD international conference on knowledge discovery & data mining*, 2018, pp. 1930–1939.
[56] P. Zhang and J. Zhang, "Memonet: Memorizing all cross features' representations efficiently via multi-hash codebook network for ctr prediction," in *Proceedings of the 32nd ACM International Conference on Information and Knowledge Management*, 2023, pp. 3154–3163.
[57] R. Wang, R. Shivanna, D. Cheng, S. Jain, D. Lin, L. Hong, and E. Chi, "Dcn v2: Improved deep & cross network and practical lessons for web-scale learning to rank systems," in *Proceedings of the web conference 2021*, 2021, pp. 1785–1797.
[58] X. Ma, L. Zhao, G. Huang, Z. Wang, Z. Hu, X. Zhu, and K. Gai, "Entire space multi-task model: An effective approach for estimating post-click conversion rate," in *The 41st International ACM SIGIR Conference on Research & Development in Information Retrieval*, 2018, pp. 1137–1140.
[59] C. Raffel, N. Shazeer, A. Roberts, K. Lee, S. Narang, M. Matena, Y. Zhou, W. Li, and P. J. Liu, "Exploring the limits of transfer learning with a unified text-to-text transformer," *Journal of machine learning research*, vol. 21, no. 140, pp. 1–67, 2020.
[60] X. Zhu, J. Li, Y. Liu, C. Ma, and W. Wang, "A survey on model compression for large language models," *arXiv preprint arXiv:2308.07633*, 2023.
[61] T. Dao, D. Fu, S. Ermon, A. Rudra, and C. Ré, "Flashattention: Fast and memory-efficient exact attention with io-awareness," *Advances in Neural Information Processing Systems*, vol. 35, pp. 16 344–16 359, 2022.
[62] R. Pope, S. Douglas, A. Chowdhery, J. Devlin, J. Bradbury, J. Heek, K. Xiao, S. Agrawal, and J. Dean, "Efficiently scaling transformer inference," *Proceedings of Machine Learning and Systems*, vol. 5, pp. 606–624, 2023.
[63] M. Zhang, H. Chen, C. Shen, Z. Yang, L. Ou, X. Yu, and B. Zhuang, "Loraprune: Pruning meets low-rank parameter-efficient fine-tuning," *arXiv preprint arXiv:2305.18403*, 2023.
[64] E. Frantar, S. Ashkboos, T. Hoefler, and D. Alistarh, "Optq: Accurate quantization for generative pre-trained transformers," in *The Eleventh International Conference on Learning Representations*, 2022.
[65] J. Lin, X. Dai, Y. Xi, W. Liu, B. Chen, H. Zhang, Y. Liu, C. Wu, X. Li, C. Zhu *et al.*, "How can recommender systems benefit from large language models: A survey," *ACM Transactions on Information Systems*, vol. 43, no. 2, pp. 1–47, 2025.
[66] Q. Pi, W. Bian, G. Zhou, X. Zhu, and K. Gai, "Practice on long sequential user behavior modeling for click-through rate prediction," in *Proceedings of the 25th ACM SIGKDD International Conference on Knowledge Discovery & Data Mining*, 2019, pp. 2671–2679.
[67] K. Ren, J. Qin, Y. Fang, W. Zhang, L. Zheng, W. Bian, G. Zhou, J. Xu, Y. Yu, X. Zhu *et al.*, "Lifelong sequential modeling with personalized memorization for user response prediction," in *Proceedings of the 42nd International ACM SIGIR Conference on Research and Development in Information Retrieval*, 2019, pp. 565–574.
[68] J. Qin, W. Zhang, X. Wu, J. Jin, Y. Fang, and Y. Yu, "User behavior retrieval for click-through rate prediction," in *Proceedings of the 43rd International ACM SIGIR Conference on Research and Development in Information Retrieval*, 2020, pp. 2347–2356.
[69] Y. Cao, X. Zhou, J. Feng, P. Huang, Y. Xiao, D. Chen, and S. Chen, "Sampling is all you need on modeling long-term user behaviors for ctr prediction," in *Proceedings of the 31st ACM International Conference on Information & Knowledge Management*, 2022, pp. 2974–2983.
[70] Z. Feng, J. Xie, K. Li, Y. Qin, P. Wang, Q. Li, B. Yin, X. Li, W. Lin, and S. Wang, "Context-based fast recommendation strategy for long user behavior sequence in meituan waimai," in *Companion Proceedings of the ACM on Web Conference 2024*, 2024, pp. 355–363.
[71] Y. Lv, S. Wang, B. Jin, Y. Yu, Y. Zhang, J. Dong, Y. Wang, X. Wang, and D. Wang, "Deep situation-aware interaction network for click-through rate prediction," in *Proceedings of the 17th ACM Conference on Recommender Systems*, 2023, pp. 171–182.
[72] J. Dong, Y. Yu, Y. Zhang, Y. Lv, S. Wang, B. Jin, Y. Wang, X. Wang, and D. Wang, "A deep behavior path matching network for click-through rate prediction," in *Companion Proceedings of the ACM Web Conference 2023*, 2023, pp. 538–542.
[73] Z. Si, L. Guan, Z. Sun, X. Zang, J. Lu, Y. Hui, X. Cao, Z. Yang, Y. Zheng, D. Leng, K. Zheng, C. Zhang, Y. Niu, Y. Song, and K. Gai, "Twin v2: Scaling ultra-long user behavior sequence modeling for enhanced ctr prediction at kuaishou," in *Proceedings of the 33rd ACM International Conference on Information and Knowledge Management*, 2024, p. 4890–4897.
[74] T. Q. Nguyen and J. Salazar, "Transformers without tears: Improving the normalization of self-attention," in *Proceedings of the 16th International Conference on Spoken Language Translation*, 2019.
[75] R. Xiong, Y. Yang, D. He, K. Zheng, S. Zheng, C. Xing, H. Zhang, Y. Lan, L. Wang, and T. Liu, "On layer normalization in the transformer architecture," in *International Conference on Machine Learning*. PMLR, 2020, pp. 10 524–10 533.